

Energy Extraction from a Kerr Black Hole - An Ultimate Power Source in the Universe?

Amir Levinson
School of Physics and Astronomy
Tel Aviv University
Tel Aviv 69978, Israel
Levinson@wise.tau.ac.il

Abstract

It is widely believed that some classes of high-energy transients may be powered by the rotational energy of a rapidly spinning black hole. The energy extraction mechanism commonly discussed involves macroscopic magnetic fields that are produced by currents flowing in a disk or torus surrounding the black hole. The discovery of relativistic jets in radio loud AGNs nearly half a century ago was the main motivation for the analysis presented in the seminal paper by Blandford and Znajek, where a global model for the magnetosphere of a Kerr black hole in the force-free limit was first constructed and employed to demonstrate that, under reasonable astrophysical conditions, energy can be extracted quite efficiently in the form of a Poynting flux. The recent discoveries of relativistic motions in Galactic microquasars, and the indications that GRBs eject ultra-relativistic, collimated outflows, have lent support to the hypothesis that this mechanism may be universal.

In spite of large efforts that have led to impressive progress in our understanding of the physics of magnetized flows in Kerr geometry, several important issues remain unresolved: the nature of the load in the Blandford-Znajek model, the causality and stability of a force free magnetosphere, global current closure, and the role of boundary conditions on the channels through which the extracted energy is released. This chapter provides an account of recent work that addresses some of those open questions. After a brief introduction, an overview of MHD in Kerr geometry will be given. The basic properties of a static black hole magnetosphere will be discussed, with particular emphasis on the conditions under which efficient energy extraction may occur. The trans-field equation that determines the geometry of magnetic flux surfaces, and the role of its critical surfaces will be summarized. The force-free limit will be considered, with an attempt to clarify several issues concerning the long standing causality problem. This will be followed by a discussion on global magnetospheric structures and related emission channels. A particular model, developed recently for the interaction of a uniformly magnetized torus with a rapidly spinning black hole under extreme conditions, those anticipated in magnetars and GRBs, will be considered in some greater detail. The magnetic field

configuration invoked in this model is vastly different from the standard one adopted in previous work, and leads to interesting astrophysical consequences that will be described in detail. In particular, the model predicts that the major fraction of the black hole spin energy should be released in the form of gravitational waves, with estimated detection rate of up to a few per year with the LIGO and VIRGO detectors. Non-stationary effects will be considered in the last part of this chapter. The requirements for local adjustments of a magnetic flux tube to temporal changes will be carefully examined, and it will be argued that changes in the angular velocity of magnetic lines induced by small disturbances, involve effects beyond the lowest order geometric optical approximation. The global evolution of a force-free magnetosphere will be explored next, with an attempt to elucidate the critical role played by the frame-dragging dynamo. Recent analytic results will be presented and contrasted with full GRMHD simulations.

1 Introduction

It is widely believed that some classes of high-energy transients, notably AGNs, microquasars, and gamma-ray bursts (GRBs), may be powered by the rotational energy of a rapidly spinning black hole. The energy extraction mechanism commonly discussed involves macroscopic magnetic fields that are produced by currents flowing in a disk or torus surrounding the black hole. A version of this idea was proposed originally by Ruffini & Wilson (1975). Blandford & Znajek (1977; henceforth BZ) were the first to construct a global model for the magnetosphere of a Kerr black hole in the force-free limit, and to demonstrate that energy can be extracted under certain conditions in the form of a Poynting flux. They applied their model to radio loud AGNs, and proposed that extragalactic jets are the consequence of this energy extraction mechanism (see review by Begelman et al. 1984). The dissipation of the Poynting flux is not addressed within the framework of the BZ model; it is merely assumed to occur in some non-force-free region where the magnetic field is sufficiently weak. The detection of prodigious gamma-ray emission from blazars by EGRET on CGRO (Thompson et al. 1993) indicates that a considerable fraction of the bulk energy is dissipated already on rather small scales. Conversion of magnetic energy to kinetic energy is a feature that appears to be common to many classes of relativistic astrophysical systems. The mechanism responsible for this process is poorly understood at present, although some ideas have been discussed (Romanova & Lovelace 1992, 1997; Levinson 1996, 1998; Thomson 1997; Levinson & van Putten 1997; Kirk & Lyubarsky 2001; Lyubarsky 2003). An important diagnostic of the BZ model is the composition of the collimated outflows, which is expected to be dominated by an electron-positron plasma. Unfortunately, the content of extragalactic as well as Galactic jets is yet an open issue (e.g., Mannheim 1993; Dermer & Shlickheiser 1993; Sikora et al. 1994; Blandford & Levinson 1995; Celotti 1997). Some constraints can be imposed from the observations (Sikora et al. 1997; Celotti

1997), but the analysis is inconclusive. This issue may be eventually resolved by the upcoming km^3 neutrino detectors. Various aspects of the BZ model have been subsequently examined in more detail by different authors (e.g., Bekenstein & Oron 1978; Macdonald & Thorne 1982; Phinney 1983; Thorne et al. 1986; Punsly & Coroniti, 1990; Ghosh & Abramovitz 1997), but many issues remained to be resolved.

The BZ model has been applied in recent years also to stellar systems, in particular GRBs (e.g., Levinson & Eichler 1993; Meszaros & Rees 1997; Van Putten 2000, 2001; Lee, et al. 2000; Brown, et al. 2000), and microquasars (Levinson & Blandford 1996). The formation of systems consisting of a rapidly rotating, stellar mass black hole surrounded by a magnetized torus, is thought to be the outcome of catastrophic events such as black hole- neutron star and neutron star-neutron star coalescence (e.g., Eichler et al. 1989; Paczyński 1991) or core collapse of massive stars (Woosley 1993). The putative existence of such black hole-torus remnants is by itself a strong motivation to consider the physics and observational consequences of the interaction of the black hole and the torus. It is quite likely that upcoming gamma-ray (e.g., MAGIC, GLAST), km^3 neutrino (e.g., Ice-Cube, NEMO), and gravitational wave (LIGO, VIRGO) detectors will detect new signatures in currently identified classes of high-energy transients, or may even discover new classes of astrophysical objects, that may be the product of the underlying black hole-torus systems. A particular example is emission of gravitational waves by a torus in suspended accretion state (Van Putten 2001, 2002; Van Putten & Levinson 2002, 2003). A key feature in this model that distinguishes it from the original BZ scenario, is a strong coupling between the black hole and the torus which is mediated by angular momentum transfer along magnetic field lines connecting the horizon and the inner face of the torus. The emission of the gravitational waves by the torus, as well as intense baryon rich winds is a consequence of this coupling. This example suggests that remnants of collapsed, massive stars may be prodigious sources of gravitational waves. The proposed association of these objects with presently known classes of GRBs (Van Putten 2001, Van Putten & Levinson 2001), is motivated in this model both phenomenologically and from theoretical considerations that imply that a small fraction of the black hole rotational energy should be expelled along the axis in the form of ultra-relativistic, baryon poor jets. However, the properties of the emission from those baryon poor jets are likely to depend also on environmental conditions and additional microphysics, and it could well be that the association with identified classes of GRBs applies only to a sub-class of these potential gravitational wave sources. Moreover, the prompt GRB emission is presumably strongly beamed, while the gravitational wave emission is roughly isotropic, so that most of those putative gravitational wave sources are not expected to be coincide with an observed GRB anyhow. On the other hand, delayed, isotropic radio emission is anticipated from the interaction of the torus winds with the ambient medium, and/or from the GRB afterglow. Systematic searches for radio transients may eventually reveal these remnants (Levinson et al. 2002). A search for associations of radio transients

with LIGO signals may provide valuable information and may aid detecting these sources.

The total amount of energy released in the BZ process depends mainly on the mass, M , and angular momentum, a , of the black hole, and the corresponding rate depends on the strength of the poloidal magnetic field threading the horizon, B . To be more precise, the Blandford-Znajek power can be expressed as (see section 2.5):

$$P_{BZ} = \epsilon \left(\frac{a}{M} \right)^2 B^2 r_H^2 c, \quad (1)$$

where $r_H = 2GM/c^2$ is the Schwarzschild radius, and ϵ is an efficiency factor that depends on the geometry of the magnetic field, as will be shown below. Typically, ϵ lies in the range $10^{-2} - 10^{-1}$. For a supermassive black hole of mass $M \sim 10^9$ solar masses, as expected in the powerful blazars, magnetic field of the order of 10^4 G is required to explain the energetics of the associated gamma-ray jets. The magnetic field may be supported by a surrounding disk and extend close to the event horizon (e.g., Bisnovatyi-Kogan & Ruzmaikin 1976). In the case of GRBs, that harbor stellar mass black holes, super-critical magnetic fields, of order 10^{15} G are needed in order to account for the characteristic luminosities measured. Such fields are much stronger than those inferred in typical radio pulsars. Which process can give rise to such amplification of the magnetic field is yet an open issue, although some models have been proposed (e.g., Thomson & Duncan 1993). Recent observational efforts provide indications of supercritical magnetic fields in magnetars (Duncan & Thompson 1992; Kouveliotou et al. 2003), suggesting that such high magnetic fields may also be present in other extreme systems.

2 IDEAL MHD IN KERR GEOMETRY

2.1 Basic equations and integrals of motion

We express the Kerr metric (Kerr 1963) in Boyer-Lindquist coordinates with the following notation:

$$ds^2 = -\alpha^2 dt^2 + \tilde{\omega}^2 (d\phi + \beta dt)^2 + \frac{\rho^2}{\Delta} dr^2 + \rho^2 d\theta^2, \quad (2)$$

where $\alpha = \rho\sqrt{\Delta}/\Sigma$ is the lapse function, $\tilde{\omega}^2 = (\Sigma^2/\rho^2)\sin^2\theta$, and $-\beta = 2aMr/\Sigma^2$ is the angular velocity of a ZAMO with respect to a distant observer, with $\Delta = r^2 + a^2 - 2Mr$, $\rho^2 = r^2 + a^2 \cos^2\theta$, and $\Sigma^2 = (r^2 + a^2)^2 - a^2\Delta \sin^2\theta$. The parameters M and a are the mass and angular momentum per unit mass of the black hole.

We denote by n , p , ρ , $h = (\rho + p)/n$, respectively, the proper particle density, pressure, energy density, and specific enthalpy of the MHD flow. The stress-energy tensor then takes the form:

$$T^{\alpha\beta} = hnu^\alpha u^\beta + pg^{\alpha\beta} + \frac{1}{4\pi}(F^{\alpha\sigma}F_\sigma^\beta - \frac{1}{4}g^{\alpha\beta}F^2), \quad (3)$$

where u^α is the four-velocity, and $F_{\mu\nu} = \partial_\mu A_\nu - \partial_\nu A_\mu$ is the electromagnetic tensor. The dynamics of the MHD system is then governed by the following set of equations: Maxwell's equations,

$$F_{;\alpha}^{\beta\alpha} = \frac{1}{\sqrt{-g}}(\sqrt{-g}F^{\beta\alpha})_{;\alpha} = 4\pi j^\beta, \quad (4)$$

$$F_{\alpha\beta;\gamma} + F_{\beta\gamma;\alpha} + F_{\gamma\alpha;\beta} = 0, \quad (5)$$

the continuity equation

$$(nu^\alpha)_{;\alpha} = \frac{1}{\sqrt{-g}}(\sqrt{-g}nu^\alpha)_{;\alpha} = 0, \quad (6)$$

and the energy and momentum equations

$$T^{\mu\nu}{}_{;\nu} = \frac{1}{\sqrt{-g}}(\sqrt{-g}T^{\mu\nu})_{;\nu} + \Gamma_{\alpha\beta}^\mu T^{\alpha\beta} = 0. \quad (7)$$

Here $\Gamma_{\alpha\beta}^\mu$ denotes the associated Cristofel symbol

In regions where the MHD flow is ideal (i.e., infinite conductivity), Ohms law yields the additional constraint,

$$u^\alpha F_{\alpha\beta} = 0. \quad (8)$$

The stationary axisymmetric flow considered here is characterized by two Killing vectors: $\xi^\mu = \partial_t$ and $\chi^\mu = \partial_\phi$. By contracting these Killing vectors with the stress-energy tensor we can construct the energy and angular momentum currents, which in Boyer-Lindquest coordinates read:

$$\mathcal{E}^r = T_\beta^r \xi^\beta = -T_t^r = -hnU^r U_t - \frac{1}{4\pi} F^{r\theta} F_{t\theta}, \quad (9)$$

$$\mathcal{E}^\theta = T_\beta^\theta \xi^\beta = -T_t^\theta = -hnU^\theta U_t + \frac{1}{4\pi} F^{r\theta} F_{tr}, \quad (10)$$

$$\mathcal{L}^r = T_\beta^r \chi^\beta = T_\phi^r = hnU^r U_\phi + \frac{1}{4\pi} F^{r\theta} F_{\phi\theta}, \quad (11)$$

$$\mathcal{L}^\theta = T_\beta^\theta \chi^\beta = T_\phi^\theta = hnU^\theta U_\phi - \frac{1}{4\pi} F^{r\theta} F_{\phi r}. \quad (12)$$

These currents are conserved, viz.,

$$\mathcal{L}_{;\alpha}^\alpha = \mathcal{E}_{;\alpha}^\alpha = 0. \quad (13)$$

The relation

$$0 = F_{\phi\theta} F_{\phi r} + F_{r\phi} F_{\phi\theta} = -(F_{\phi\theta} \partial_r + F_{r\phi} \partial_\theta) A_\phi \equiv D_\psi A_\phi, \quad (14)$$

where the operator $D_\psi = F_{\theta\phi} \partial_r + F_{\phi r} \partial_\theta$ denotes derivative along magnetic flux surfaces, implies that A_ϕ is conserved on magnetic flux surfaces and is, therefore, a

viable stream function. We can use the dual electromagnetic tensor, denoted here by $\mathcal{F}^{\mu\nu}$, to express the invariant $\mathbf{E} \cdot \mathbf{B}$ in the form,

$$\mathbf{E} \cdot \mathbf{B} = -(\sqrt{-g}/4)\mathcal{F}^{\mu\nu}F_{\mu\nu} = D_\psi A_t. \quad (15)$$

It can be readily shown that the ideal MHD condition, given by eq. (8), implies that $\mathbf{E} \cdot \mathbf{B} = 0$, meaning that the electric potential is conserved along magnetic surfaces. We note that in cases where a gauge $A_t = -\Omega A_\phi$ can be found, where $\Omega(r, \theta)$ is some function of the coordinates, the change in the electric potential along flux surfaces is given by $D_\psi A_t = -A_\phi D_\psi \Omega$, where eq. (14) has been used. Thus, in regions where the MHD flow is ideal Ω is conserved along magnetic surfaces. As discussed below the function Ω is approximately the angular velocity of the magnetic flux tube at small angles. On the other hand, in regions where the ideal MHD condition is violated, e.g., the sparking gap (see below), the change in angular velocity across this region is related to the electric potential drop through: $\Delta A_t = -A_\phi \Delta \Omega$ (note that in steady-state A_ϕ is conserved even in the non-ideal case). The relevancy of this result to the double transonic flow is discussed below.

Equations (5), (6), (8), and (9)-(13) admit four additional quantities that are conserved along magnetic flux surfaces (e.g., Bekenstein & Oron 1978): The particle flux per unit magnetic flux,

$$\eta(\Psi) = \frac{\sqrt{-g}nu^r}{F_{\theta\phi}} = \frac{\sqrt{-g}nu^\theta}{F_{\phi r}}; \quad (16)$$

the angular velocity of magnetic field lines,

$$\Omega_F(\Psi) = -\frac{\eta}{\sqrt{-g}nu^t}F_{r\theta} + v^\phi; \quad (17)$$

and the total energy and angular momentum per particle carried by the MHD flow,

$$E(\Psi) = -hu_t - \frac{\sqrt{-g}}{4\pi\eta}\Omega_F F^{r\theta}, \quad (18)$$

$$L(\Psi) = hu_\phi - \frac{\sqrt{-g}}{4\pi\eta}F^{r\theta}. \quad (19)$$

Here $v^\phi = u^\phi/u^t$, and $v^r = u^r/u^t$ are the corresponding components of the 3-velocity. The fifth integral of motion is the entropy $s = s(\Psi)$. Equations (16)- (19) can be solved for u_t , u_ϕ and $F^{r\theta}$. The solution can then be used to express F_θ^r , $u^t = g^{tt}u_t + g^{t\phi}u_\phi$, and $u^\phi = g^{\phi t}u_t + g^{\phi\phi}u_\phi$ as:

$$F_\theta^r = -\frac{4\pi\eta}{\sin\theta} \frac{\alpha^2 L - \tilde{\omega}^2(\Omega_F + \beta)(E + \beta L)}{\alpha^2 - \tilde{\omega}^2(\Omega_F + \beta)^2 - M^2}, \quad (20)$$

$$hu^t = \frac{1}{\alpha^2} \frac{\alpha^2(E - \Omega_F L) - M^2(E + \beta L)}{\alpha^2 - \tilde{\omega}^2(\Omega_F + \beta)^2 - M^2}, \quad (21)$$

$$hu^\phi = \frac{\alpha^2 \tilde{\omega}^2 \Omega_F (E - \Omega_F L) + \tilde{\omega}^2 \beta M^2 (E + \beta L) - \alpha^2 M^2 L}{\alpha^2 \tilde{\omega}^2 [\alpha^2 - \tilde{\omega}^2 (\Omega_F + \beta)^2 - M^2]}, \quad (22)$$

where $M^2 = (4\pi h\eta^2)/n$. The meaning of the latter becomes clear when written in terms of ZAMO 4-velocities. By employing eq. (16) one obtains $M^2 = \alpha^2 u_p^2 / u_A^2$, where $u_p = (u^r u_r + u^\theta u_\theta)^{1/2}$ and $u_A = (B_p^2 / 4\pi h n)^{1/2}$, with $B_p^2 = (\Sigma \sin \theta)^{-2} (F_{\phi\theta}^2 + \Delta F_{\phi r}^2)$, are, respectively, the poloidal velocity and Alfvén velocity, as measured by a ZAMO (see e.g., Macdonald & Thorne 1982, Beskin 1997). Thus, M is up to a factor α the Alfvén Mach number. Finally, using the normalization condition, $u^\mu u_\mu = -1$ and the definition of the Mach number M , we obtain the Bernoulli equation

$$u_p^2 + 1 = \frac{M^4 B_p^2}{16\pi^2 \eta^2 \alpha^2 h^2} + 1 = (\alpha u^t)^2 - \tilde{\omega}^2 (\beta u^t + u^\phi)^2. \quad (23)$$

Note that since the enthalpy h is a function of the thermodynamic variables n and s only, the density and enthalpy can be expressed in terms of s and M , viz., $n = n(s, M)$, $h = h(s, M)$. Thus, equations (20)-(23) determine essentially all the flow characteristics in terms of the five integrals of motion once the poloidal magnetic field is known.

2.2 Asymptotic behavior of the MHD flow

Consider first the behavior of the solution near the horizon. There $\alpha \rightarrow 0$, and for physical solutions for which the Mach number is finite on the horizon, $M(r_H) \neq 0$, eqs. (21) and (22) yield $u^\phi \rightarrow \Omega_H u^t$ as $\alpha \rightarrow 0$, where $\Omega_H = -\beta_H$ is the angular velocity of the black hole. Consequently, the rotation of the plasma on the horizon is synchronous with the black hole, as one might expect. Substituting the latter result into Bernoulli equation (23), we obtain $u_p \rightarrow \alpha u^t$ on the horizon. The poloidal velocity is radial on the horizon, implying $u_p^2 \rightarrow g_{rr} u^r u^r$, hence

$$v^r = u^r / u^t \rightarrow \alpha / \sqrt{g_{rr}} = -\Delta / (r^2 + a^2). \quad (24)$$

This shows that the plasma moves along geodesics of a freely falling observer as it approaches the horizon, meaning that near the horizon the dynamics is governed by gravity alone. Substituting v^ϕ and v^r obtained above into eqs. (16) and (17), yields

$$\frac{F_{r\theta}}{F_{\phi\theta}} = -\frac{r^2 + a^2}{\Delta} (\Omega_F - \Omega_H). \quad (25)$$

Eq. (25) gives the frozen-in condition derived originally by Znajek (1977) and used by BZ as a boundary condition in their force-free analysis.

Next, consider the behavior of a MHD outflow far from the black hole. The outflow parameters are given, to a good approximation, by eqs (20)-(23) with $\alpha^2 = 1$, $\beta = 0$. At the Alfvén surface the Mach number is $M_A^2 = 1 - \tilde{\omega}_A^2 \Omega_F^2$, and the requirement that $F_\theta^r u^t$ and u^ϕ remain finite there yields the well known relation $L/E = \tilde{\omega}_A^2 \Omega_F$ (e.g., Weber & Davis 1967; Camenzind 1986). By employing eqs. (16) and (17) we obtain,

$$\frac{F_{r\theta}}{F_{\phi\theta}} = -\frac{M^2 (R^2 \Omega E - L)}{R^2 v^r [(1 - M^2) E - \Omega L]} = \frac{(\tilde{\omega}^2 - \tilde{\omega}_A^2) M^2 \Omega_F}{v^r \tilde{\omega}^2 (M^2 - M_A^2)}. \quad (26)$$

Well above the Alfvén point, where $\tilde{\omega} \gg \tilde{\omega}_A$ and $M \gg M_A$ the last equation gives

$$\frac{F_{r\theta}}{F_{\phi\theta}} \rightarrow \frac{\Omega_F}{v^r}. \quad (27)$$

The asymptotic poloidal current follows from the r component of eq. (4):

$$\frac{\partial}{\partial\theta} \left(\frac{\Delta \sin\theta}{\rho^2} F_{r\theta} \right) = 4\pi\sqrt{-g}j^r. \quad (28)$$

Integrating the latter equation we obtain the net electric current within a flux tube,

$$I = \int 2\pi\sqrt{-g}j^r d\theta = \frac{\Delta \sin\theta}{2\rho^2} F_{r\theta}. \quad (29)$$

Using eqs (25) and (27) we find that the net electric current flowing on the horizon is given by

$$I_H = \frac{\Sigma \sin\theta}{2\rho^2} (\Omega_H - \Omega_F) F_{\phi\theta}, \quad (30)$$

and the net electric current at infinity is given by,

$$I_\infty = \frac{\Omega_F}{2v^r} \sin\theta F_{\phi\theta}, \quad (31)$$

2.3 Conditions for energy extraction by a magnetized inflow

Detailed analysis of the inflow structure and the requirements for extraction of the hole rotational energy is given in Takahashi et al. (1990) and Hirotani et al. (1992). For completeness, we give in this section a brief derivation of the conditions under which energy extraction by a MHD inflow is possible. From equations (9)-(12), (18) and (19) it is readily seen that the energy and angular momentum fluxes can be expressed as: $\mathcal{E}^a = E n u^a$, and $\mathcal{L}^a = L n u^a$, with $a = r, \theta$. Here $n u^a$ is the particle flux carried by the MHD flow. Consequently, energy extraction by the MHD inflow (for which $n u^a$ is negative) then requires the specific energy to be negative, viz., $E(\psi) < 0$. This shows that the BZ mechanism is indeed a manifestation of the Penrose process, as pointed out by Takahashi et al. (1990)

Now, at the Alfvén surface the denominator of eqs (20)-(22) vanishes, and we obtain

$$M_A^2 = \alpha_A^2 - \tilde{\omega}_A^2 (\Omega_F + \beta_A)^2 \geq 0, \quad (32)$$

where the subscript A refers to quantities on the Alfvén surface. This in turn implies that the angular velocity of magnetic field lines must lie in the range

$$-\beta_A - \alpha_A/\tilde{\omega}_A < \Omega_F < -\beta_A + \alpha_A/\tilde{\omega}_A. \quad (33)$$

In order for u^t to be finite on the Alfvén surface, the relation

$$\frac{L}{E} = \frac{\tilde{\omega}_A^2 (\Omega_F + \beta_A)}{\alpha_A^2 - \tilde{\omega}_A^2 \beta_A (\Omega_F + \beta_A)} \quad (34)$$

must hold (see eq. [21]). At the injection surface of the inflow we take $M^2 \sim 0$. Equation (23) then yields

$$E - \Omega_F L = h_{inj}[\alpha_{inj}^2 - \tilde{\omega}_{inj}^2(\Omega_F + \beta_{inj})^2]^{1/2} \geq 0. \quad (35)$$

Solving eqs (34) and (35) we obtain

$$E = \frac{\alpha_A^2 - \tilde{\omega}_A^2 \beta_A (\Omega_F + \beta_A)}{\alpha_A^2 - \tilde{\omega}_A^2 (\Omega_F + \beta_A)^2} h_{inj} [\alpha_{inj}^2 - \tilde{\omega}_{inj}^2 (\Omega_F + \beta_{inj})^2]^{1/2}, \quad (36)$$

$$L = \frac{\tilde{\omega}_A^2 (\Omega_F + \beta_A)}{\alpha_A^2 - \tilde{\omega}_A^2 (\Omega_F + \beta_A)^2} h_{inj} [\alpha_{inj}^2 - \tilde{\omega}_{inj}^2 (\Omega_F + \beta_{inj})^2]^{1/2}. \quad (37)$$

Evidently, the specific energy will be negative provided the condition $\alpha_A^2 - \tilde{\omega}_A^2 \beta_A (\Omega_F + \beta_A) < 0$ is satisfied on the Alfvén surface. The latter condition combined with eq. (33) implies, in turn, that the rotational energy of the hole can be extracted only if (i) the Alfvén surface of the inflow is located inside the ergosphere, and (ii) $0 < \Omega_F < \Omega_H$.

2.4 The trans-field equation

Equation (16) can be used to express the poloidal components of the 4-velocity in terms of the magnetic field components. Substituting the latter into eq. (3), the poloidal components of the stress-energy tensor can be written as:

$$T^{ab} = \frac{M^2}{16\pi^2(\sqrt{-g})^2} (\partial_a \psi)(\partial_b \psi) - pg^{ab} + \frac{1}{4\pi} (F^{\alpha\sigma} F_\sigma^\beta + \frac{1}{4} g^{\alpha\beta} F^2), \quad (38)$$

where $\psi = 2\pi A_\phi$ is the magnetic flux, and the indices a, b run through r and θ only. The poloidal magnetic and electric fields in eq. (38) are given in terms of the stream function ψ as: $F_{\phi a} = -(1/2\pi)\partial_a \psi$, $F_{ta} = -\Omega_F F_{\phi a}$, and the toroidal magnetic field $F_{r\theta}$ by eq. (20). Upon substituting eq. (38) into eq. (7), one obtains a second order PDE for the stream function ψ , involving the five integrals of motion, the Mach number, the proper density n and the temperature. The resultant trans-field equation is given explicitly in eq. (39) of Beskin (1997)¹. Combined with Bernoulli equation (23) and an appropriate equation of state, that allow one to express, though implicitly, the Mach number and the thermodynamic parameters in terms of the conserved quantities, this trans-field equation can be solved in principle to yield the stream function, $\psi = \psi(r, \theta)$, for a given set of boundary conditions. The functional form of the invariants $\Omega(\psi)$, $L(\psi)$, $E(\psi)$, $\eta(\psi)$ and $s(\psi)$ that appear explicitly in the equation must be specified first through appropriate boundary conditions.

The trans-field equation has, in general, several singular surfaces. Those singular surfaces can be identified from differentiation of eq. (23), whereby an expression for

¹The trans-field equation is written in Beskin 1997, who uses the 3+1 formalism, in terms of the operator $\nabla = \hat{e}_r \sqrt{\Delta\rho}^{-1} \partial_r + \hat{e}_\theta \rho^{-1} \partial_\theta$

the gradient of the Mach number can be obtained (Takahashi 1990; Beskin 1997). Of most interest are the Alfvén surface², on which the Mach number satisfies relation (32) and the fast and slow magnetosonic surfaces on which the poloidal 4-velocity satisfies

$$u_p^2 = K \pm \sqrt{K^2 - 4c_s^2 u_A^2 [1 - (\Omega_F + \beta)^2 \tilde{\omega}^2 \alpha^{-2}]}, \quad (39)$$

with the + (−) sign applies to the fast (slow) magnetosonic surface. Here $2K = [1 - (\Omega_F + \beta)^2 \tilde{\omega}^2 \alpha^{-2}] u_A^2 + (B_\phi^2 / 4\pi h n) + c_s^2$, where $B_\phi = (\sqrt{\Delta} / \rho^2) F_{r\theta}$ is the ZAMO toroidal magnetic field, and c_s is the sound 4-velocity, given by $c_s^2 = a_s^2 / (1 - a_s^2)$ with $a_s^2 = (1/h)(\partial p / \partial n)_s$. As the flow accelerates, it crosses first the slow surface, then the Alfvén surface, next the light cylinder, and finally the fast surface. As shown in e.g., Beskin (1997), with the exception of the force-free case the trans-field equation changes from elliptic to hyperbolic on the fast critical surface, meaning that the flow beyond that surface (between the fast critical surface and the horizon in the inflow section) is not in causal contact with the region between the fast critical surface and the injection point. In the force-free limit discussed next, the Alfvén surface coincides with the light cylinder, and the fast critical surface with the horizon. In this case the trans-field equation remains elliptic down to the horizon. Now, the requirement that the MHD flow pass smoothly through the critical surface imposes certain relations between the conserved quantities of the MHD flow. Since the trans-field equation is second order the number of boundary conditions required is 2 + number of conserved quantities - number of singular surfaces.

There is ample literature on the properties of the Grad-Shafranov equation and its solutions in flat spacetime, mainly in the context of pulsar physics (see e.g., Mestel 1999, and references therein). Solutions of the trans-field equation in curved spacetime were obtained in various limits. Examples are discussed in, e.g., (Blandford & Znajek 1977; Fendt 1997; Beskin 1997; Ghosh 2000; Beskin & Kuznetsova 2000; Lee, et al. 2001; Uzdensky 2004a,b)

2.5 The force-free limit

In situations where the MHD flow is so highly magnetized that the inertia of the plasma can be ignored, the system approaches the force-free limit. Formally this limit can be obtained by setting $h \rightarrow 0$ in the above equations³. This in turn implies $M^2 \rightarrow 0$ (meaning essentially that the Alfvén velocity, as measured by a ZAMO, approaches the speed of light). The Alfvén surface then approaches the light cylinder, as can be readily seen from eq. (32). In the limit $h = 0$ eq. (7)

²It is noteworthy that although the Grad-Shafranov equation has a singularity on the Alfvén surface, the regularity of equations (20)-(22) is automatically satisfied. It merely defines the location of this surface.

³We note that in reality $h \geq mc^2$, where m is the rest mass of a particle in the flow. The limit $M^2 \ll 1$ is due to the small particle density. Thus, the limit of negligible inertia is better characterized by the dimensionless Mach number.

reduces to

$$F_{\mu\nu}j^\nu = 0, \quad (40)$$

where eq. (4) has been used. The toroidal component of the last equation and the condition $F_{\phi t} = 0$ give $F_{\phi r}j^r + F_{\phi\theta}j^\theta = 0$, meaning that the poloidal current must flow along magnetic flux surfaces. Consequently, the net electric current within a given flux surface, given by eq. (29), is conserved, as can be readily verified by using the r and θ components of eq. (4) and the latter condition.

The total energy and angular momentum are given by $E_{tot} = \eta E$ and $L_{tot} = \eta L$. By employing eqs. (18) and (19) we obtain $E_{tot} = \Omega_F L_{tot}$ (to be more precise, eq. [35] shows that this result is correct, in general, to order $h_{inj}\eta$). Taking the limit $M^2 \rightarrow 0$ and $E \rightarrow \Omega_F L$ in eq. (20) and using eq. (29) we also find $I = 2\pi L_{tot}$. Thus, the force-free system has only two integrals of motion, Ω_F and I .

Combining eqs (9) and (25), one can obtain the energy flux on the horizon:

$$\mathcal{E}^r = \Omega_F(\Omega_H - \Omega_F) \frac{\Sigma}{\rho^4} (F_{\phi\theta})^2, \quad (41)$$

which is a well known result, derived originally by BZ. Maximum extraction efficiency occurs for $\Omega_F = \Omega_H/2$. The net power transferred outwards from the horizon is $P = 2\pi \int \sqrt{-g} \mathcal{E}^r d\theta$, where the integration is over the horizon surface. By expressing $F_{\phi\theta}$ in terms of the ZAMO poloidal field, $B_r = -F_{\phi\theta}/\Sigma \sin\theta$, in eq. (41), and scaling the metric components, we arrive at eq. (1), with the dimensionless factor ϵ given explicitly as an integral involving the scaled components.

2.6 The Double transonic flow

In many applications of the BZ mechanism to astrophysical systems it is envisioned that the energy extracted near the horizon of the hole is ultimately transferred to large radii in the form of a relativistic jet. Since the poloidal velocity of the outflowing plasma is in the opposite direction to that of the negative energy inflow inside the ergosphere, the invariants $\eta(\psi)$, $E(\psi)$ and $L(\psi)$ must have an opposite sign in the two regions (the energy and angular momentum fluxes can be continuous nonetheless), implying that there must exist a region, that we shall term the injection region, where the ideal MHD condition is violated, and where fresh plasma is produced. This region must be located somewhere between the inner and outer Alfvén surfaces (Takahashi et al. 1990). We point out that this discontinuity in the flow does not appear implicitly in the force-free case, where formally $\eta = 0$. As shown above, the force-free system has only two invariants, I and Ω , both of which can be assumed continuous in the entire region between the inner and outer fast magnetosonic surfaces. The implicit assumption being made is that there exists a source of electric charges, presumably located on the neutral surface defined below.

For illustration let us consider the properties of the double transonic flow near the rotation axis of the black hole (figure 1). We suppose that the MHD inflow

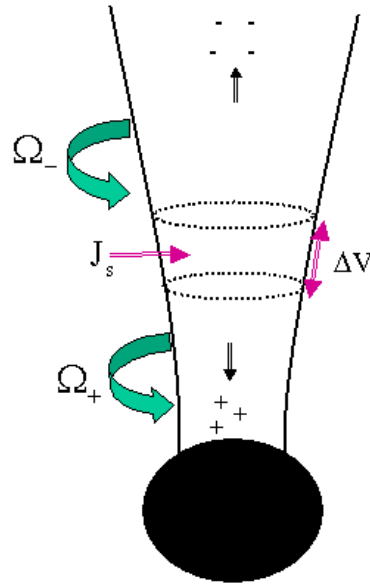


Figure 1: Schematic illustration of a double-transonic structure. Transonics inflow and outflow are expelled from the injection region where plasma is continuously generated. Magnetic flux surfaces are assumed to be continuous across the injection region. The angular velocities of magnetic field lines in the inflow and outflow sections are determined by the potential drop ΔV along magnetic surfaces in the injection region, and the cross-field electric current $J_s = I_H - I_\infty$ (see text).

and outflow expelled from the injection region become ideal outside the injection region. The entire system is then characterized by 10 invariants, 5 for each flow. We henceforth refer to quantities in the inflow (outflow) by a subscript + (-). Consider first the charge distribution near the axis. The t component of eq. (4) reduces in the small angle approximation to,

$$\frac{\partial}{\partial \theta} \left[\frac{\sin \theta}{\alpha^2} (\Omega + \beta) F_{\phi\theta} \right] = 4\pi \sqrt{-g} j^t. \quad (42)$$

For reasonable magnetic field configurations eq. (42) can be integrated to yield the lowest order Goldreich-Julian charge density:

$$j^t = -\frac{(\Omega_F + \beta) B_r}{2\pi \alpha^2}, \quad (43)$$

where B_r is the ZAMO radial magnetic field. As seen, the charge density changes sign across a neutral sheet on which the angular velocity of magnetic lines, as measured by a ZAMO is zero, viz., $\Omega_F = -\beta$. Now, to lowest order eqs. (30) and (31) give

$$I_H(\psi) = -\frac{(\Omega_H - \Omega_+) \psi}{2\pi}, \quad (44)$$

$$I_\infty(\psi) = -\frac{\Omega_- \psi}{2\pi}. \quad (45)$$

Assuming that the stream function is continuous across the injection region then implies that an amount

$$\Delta I = I_H - I_\infty = -\frac{(\Omega_H - \Omega_+ - \Omega_-) \psi}{2\pi} \quad (46)$$

of cross-field electric current must be supplied into the flux tube. In situations where inertia is negligible, so that the inflow and outflow can be considered force-free, the current ΔI must be supplied by the injection region. Under the assumption that the stream function is continuous a gauge can be found such that $A_t \simeq -\psi/2\pi$ to lowest order. The potential drop along magnetic flux tubes in the injection region is then given by (see eq [15] and the text below),

$$\Delta V = -(\Omega_+ - \Omega_-) \psi / 2\pi. \quad (47)$$

Once a solution $\psi(r, \theta)$ of the Grad-Shafranov equation is found, eqs. (46) and (47) can be solved to yield the angular velocity of magnetic field lines on the horizon near the axis in terms of the magnetic flux, cross field current, and potential drop in the injection region:

$$\Omega_+ = \frac{1}{2} \left[\Omega_H + \frac{2\pi(\Delta I - \Delta V)}{\psi} \right]. \quad (48)$$

In general, ΔI and ΔV will be determined by the conditions in the injection region. Consequently, the angular velocity of magnetic lines on the horizon and, hence, the efficiency at which energy is extracted from the hole are determined by the microphysics of the injection region. The values of ΔV and ΔI , the toroidal electric current in the interface separating the inflow and outflow, and the continuity of the stream function across this interface provide 4 boundary conditions for the Grad-Shafranov equation governing the structure of the double transonic flow. The values of the injected densities, $n_{inj\pm}$, enthalpies, $h_{inj\pm}$, and poloidal velocities, $u_{p\pm}|_{inj}$, provide the six additional boundary conditions required. Thus, it seems that the entire structure is determined essentially by the physical conditions in the injection region and the regularity conditions at the critical surfaces alone. No additional boundary conditions are required on the horizon. This remains true in the limit of very small (albeit finite) inertia. In particular, when $\Delta I \ll I_{GJ}$ and $\Delta V \ll V_{max}$, as expected in situations whereby the plasma source is associated with a quasi-steady sparking gap, inside which the field aligned electric field $E_{||}$ is almost completely screened out, we obtain $\Omega_+ \simeq \Omega_H/2$ near the axis, confirming earlier results (Blandford & Znajek 1977, Phinney 1983). Detailed analysis of a perturbed split monopole solution for a double transonic flow is presented in Beskin & Kuznetsova (2000), who reached similar conclusions.

2.7 Inflow from a uniformly magnetized, massive torus

As a second example we consider a situation in which the magnetic field lines extending from the horizon are anchored to a massive torus. This is shown schematically in figure 2. We suppose that the mass flux along field lines connecting the torus and the black hole is small, and approximate the inflow as force-free. This may be justified in cases where angular momentum transfer from the hole to the torus results in a slightly super-Keplerian rotation of the inner parts of the torus, thereby strongly suppressing accretion (van Putten & Ostriker 2001).

For an infinitely conducting torus, the angular velocity of magnetic field lines that originate from the torus equals the the angular velocity of the torus, viz., $\Omega_F = \Omega_T$. The torque exerted on the inner face of the torus by the black hole is obtained by integrating the angular momentum flux \mathcal{L}^r given by eq. (11) over the section of the horizon which is threaded by magnetic field lines that are anchored to the torus:

$$\tau = -4\pi \int_{\theta_H}^{\pi/2} \sqrt{-g} \mathcal{L}^r d\theta = (\Omega_H - \Omega_T) \int_{\theta_H}^{\pi/2} \frac{\Sigma}{\rho^2} \sin \theta (F_{\phi\theta})^2 d\theta, \quad (49)$$

where eq. (25) has been used. Here θ_H is the angle of the last field line that connects the torus and the horizon. In terms of the net poloidal magnetic flux associated with the open field lines in the torus, ψ_0 , we may write $\tau = (\Omega_H - \Omega_T) f_H^2 \psi_0^2 / 4\pi$. Formally f_H is defined through eq. (49). It roughly represents the fraction of surface area of the horizon that is threaded by magnetic field lines emerging from the torus.

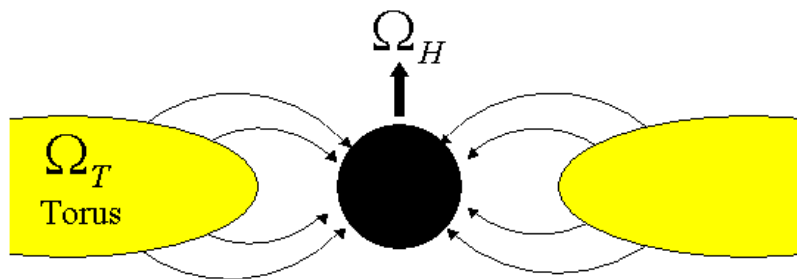


Figure 2: Inflow from a massive, infinitely conducting torus: In this example there is a direct link between the torus and the black hole. The angular velocity of magnetic field lines that penetrate the horizon equals Ω_T . Energy and angular momentum are transferred from the black hole to the torus when $\Omega_H > \Omega_T$, and in the opposite direction when $\Omega_H < \Omega_T$.

It is seen that when $\Omega_H > \Omega_T$ angular momentum is transferred from the black hole to the torus, tending to spin up the inner face, whereas in the slowly rotating case ($\Omega_H < \Omega_T$) the black hole receives angular momentum from the torus. The associated power is given simply by $L = \Omega_T \tau$.

2.8 Is there a causality problem?

The question whether a force-free magnetosphere can exist and whether it is stable has been the subject of a long debate (Punsly & Coroniti 1990, Beskin & Kuznetsova 2000; Komissarov 2001,2003,2004b; Blandford 2001, 2002; Punsly 2003, 2004 van Putten & Levinson 2003; Levinson 2004). In particular it has been argued that a force-free black hole magnetosphere is not a causal structure and, therefore, physically excluded. The claim made by Punsly and collaborators is that the fact that the angular velocity, Ω_F , of a force-free flux tube extending from the horizon is not a free parameter, but is determined by matching boundary conditions on the horizon and at infinity (as in the analysis of BZ and Phinney 1983) violates the principle of MHD causality. The reason is that the inflowing magnetic wind must pass through the inner light cylinder before reaching the horizon and, therefore, cannot communicate with the plasma source region (see section 4.1). Their main conclusion is that the use of the Znajek frozen-in condition on the horizon to determine Ω_F is unphysical, and that Ω_F must be determined by the dissipative process that leads to ejection of plasma on magnetic field lines between the inner and outer Alfvén points. This view seems to follow from the interpretation of the membrane paradigm, that the horizon can be viewed as a conducting surface (see also Komissarov 2004b). It has already been emphasized in the preceding section that the Grad-Shafranov equation is in general hyperbolic near the horizon and requires no boundary conditions there, and that the Znajek frozen-in condition is essentially a regularity condition on the fast critical surface. Moreover, it has been argued that the injection region alone determines the entire solution of the double transonic flow. The question whether a force-free magnetosphere is stable and how it evolves is nonetheless relevant. Blandford (2001, 2002) suggested that any changes are communicated by means of a fast magnetosonic mode, that can propagate across magnetic field lines at the speed of light and carry information about the toroidal magnetic field and poloidal current to the plasma source even beyond the light cylinder. Punsly (2003) argued that the fast mode can only carry displacement currents, and therefore concluded that fast characteristics cannot transmit sufficient information to affect the global structure. Levinson (2004) in turn claimed that to second order the fast mode can affect the poloidal current (see section 4.1 below for further details). The present view of this author, as explained below, is that although this is an interesting issue, it is of little relevancy to the causality problem.

To elucidate how a force-free magnetosphere responds to changes in spacetime, consider the following Gedanken experiment. Suppose that a double transonic flow has been ejected along the rotation axis of a Kerr black hole, and assume further that

the flow is force-free everywhere except for the plasma source region where a small deviation from force-freeness must exist. Imagine now that the angular momentum of the hole changes abruptly at time t_0 from a_0 to $a_0 + \delta a$. This will induce a change $-\delta\beta(r)$ in the angular velocity of a ZAMO at any radius r . The question then is how this variation in space-time would affect the flow. From eq. (43) it is evident that a change

$$\delta j^t(r) = -\frac{(\delta\Omega_F + \delta\beta)B_r}{2\pi\alpha^2} \quad (50)$$

in the local electric charge density near the axis is required in order for the MHD flow to remain ideal, where $\delta\Omega_F$ is the resultant change in the angular velocity of the magnetic flux tube. This is particularly true in the region between the inner Alfvén and fast critical surfaces. Whether the charge density adjusts by means of second order effects of the fast mode, as suggested by Levinson (2004; but cf. Punsly 2004), or otherwise is an interesting question by its own. In our view it must adjust. The crucial point is that any deviation of j^t from the Goldreich-Julian value will induce a field-aligned electric field (i.e., $\mathbf{E} \cdot \mathbf{B} \neq 0$), in violation of the force-free assumption, that would tend to be screened out instantaneously by the surrounding plasma. Such a process involves most likely generation of longitudinal modes that cannot be analyzed within the framework of force-free wave analysis anyhow. Whether a quasi steady-state can be maintained in such a case is unclear to this author. Recent time-dependent analysis of sparking gaps demonstrates that a response of this kind might be oscillatory in nature (Levinson et al., in preparation). The analysis outlined in section 4.2 demonstrates that the magnetosphere remains force-free during the course of evolution provided that sufficient plasma is present on field lines.

Now, if conditions in the plasma source are such that it always tends to be sustained in an approximately force-free state, in the sense that the cross field current ΔI and the potential drop across the plasma source region ΔV are negligibly small, then it follows from eqs. (30) and (31) that as long as $\Omega_F \neq (\Omega_H + \delta\Omega_H)/2$, the charge density in the gap will change with time since $\vec{\nabla} \cdot \vec{j} \neq 0$. This will feedback on the potential drop ΔV , and will lead to an evolution of the poloidal current and, hence, Ω_F , until the value $(\Omega_H + \delta\Omega_H)/2$ is exceeded⁴.

3 THE GLOBAL STRUCTURE

The global structure of the magnetosphere determines the geometry of magnetic flux surfaces and the location of regions where substantial departure from ideal MHD takes place. The existence of such regions is essential in order to allow for (i) cross-field currents that are necessary for global current closure, and (ii) dissipation of magnetic energy to account for the high entropy inferred in most astrophysical

⁴This assumes again that the system can relax to a steady-state. Alternatively, it may undergo large amplitude oscillations.

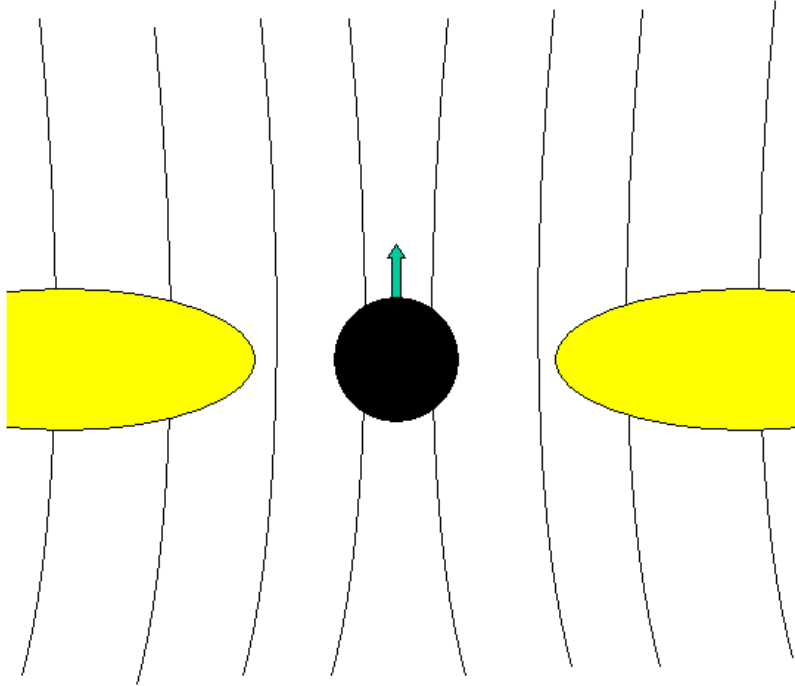


Figure 3: Schematic representation of an open-field magnetosphere

applications. Moreover, the global structure determines through which channels the BH rotational energy extracted is emitted.

In most astrophysical applications it is envisioned that the magnetic field threading the horizon is supported by currents flowing in a disk or torus surrounding the black hole. Two inherently different disk magnetizations are discussed in the literature. The first one consists of what we term an open-field magnetosphere. In the second one, termed closed-field geometry, a large portion of magnetic field lines that thread the horizon are anchored to the torus (Nitta et al. 1991; van Putten 1999, 2001; Uzdensky 2004b). This introduces a strong coupling between the black hole and the torus. In what follows we discuss those two magnetospheric configurations in some greater detail.

3.1 Open-Field Geometry

This configuration has been studied extensively (e.g., Blandford 1976; Lovelace 1976; Phinney 1983; Macdonald 1984; Beskin & Par v 1993), and was the one employed originally by BZ in their model. It is shown schematically in fig 3. In this config-

uration there is no direct link between the horizon and the disk. In particular, all field lines that penetrate the horizon extend to infinity. The energy extracted from the hole is then transported outward to the load along those field lines in the form of a Poynting flux. The nature of the load, where magnetic energy is presumably being converted to kinetic energy, is not well understood at present. The current closure path is also not well understood. It is conceivable that a current sheet may form on the equatorial plane, thereby providing a return path. This idea seems to be supported by recent numerical simulations (Komissarov 2004b). If so, then a torque may be exerted on the inner parts of the disk by the cross-field currents. This may give rise to enhanced dissipation, which has been claimed to be inferred recently from X-ray observations of MCG-6-30-15 (Wilms, et al. 2001). However, rapid heating of the inner parts of the disk are expected also in the closed-field magnetosphere, though for a different reason as explained below.

3.2 Closed-Field Geometry

The basic properties of such a magnetosphere can be illustrated by matching a vacuum solution to a uniformly magnetized torus. Such a solution is topologically equivalent to a configuration produced by two counter-oriented current rings in the equatorial plane, which in flat space-time can be calculated analytically. The resultant magnetic flux surfaces of this vacuum solution are exhibited in fig. 4. A third current loop associated with the black hole equilibrium magnetic moment in its lowest energy state (van Putten 2001) has been added in the figure. It is oriented antiparallel to the surrounding torus magnetosphere, facilitating an essentially uniform and maximal horizon flux at arbitrary spin-rates. It only affects the solution very near the horizon. As seen, there are two separated regions of closed field lines. At large radii (compared with the radius of the outer current ring) the field quickly approaches a dipole solution. In the inner region the field lines intersect the horizon, giving rise to a strong coupling between the black hole and the inner face of the torus.

Now, the magnetic field inside the torus cannot be purely poloidal, because purely poloidal fields are unstable and tend to decay completely in a few Alfvén timescales (Markey & Tayler, 1973; Flowers & Ruderman, 1975; Eichler 1982). However, by conservation of helicity, a twisted magnetic field does not decay to zero, at least in the limit of ideal magnetohydrodynamics. Instead, it will evolve into a new, stable configuration. Recent 3D MHD simulations (Braithwaite & Spruit, 2004) show that magnetic fields inside stars tend to develop a belt of twisted field lines that stabilize a dipolar field in the magnetosphere above the stellar surface. This configuration appears to be stable over the resistive timescale, which is typically much longer than the canonical dynamical timescales (e.g., rotation periods and acoustic timescales). By topological equivalence in poloidal cross-section, it is therefore conceivable that the magnetic field inside the torus is twisted as well, supporting an overall torus magnetosphere which, from the outside, is consistent

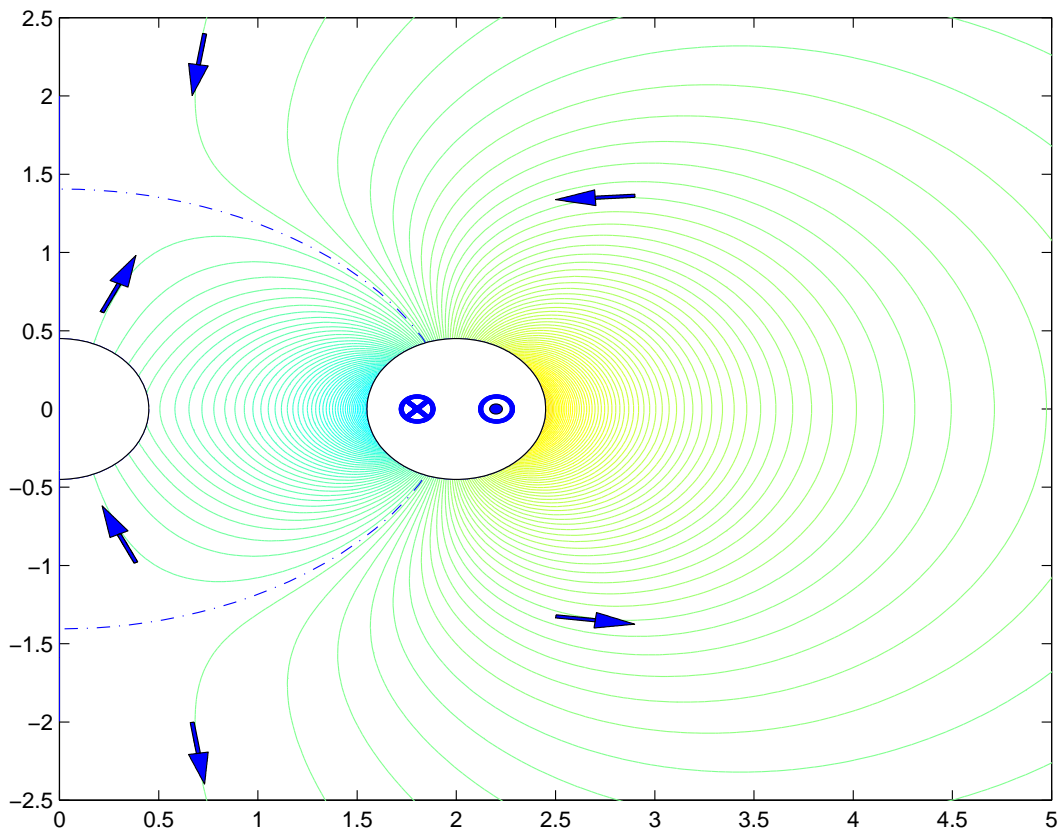


Figure 4: The poloidal topology of magnetic flux-surfaces in vacuum produced by two counter-oriented current rings is shown. The current rings are located on the equatorial plane, one on the side of the torus facing the black hole and the other one on the opposite side, as indicated. The dashed line is the separatrix between the flux-surfaces supported by the inner and the outer faces of the torus. Reprinted from van Putten (2004).

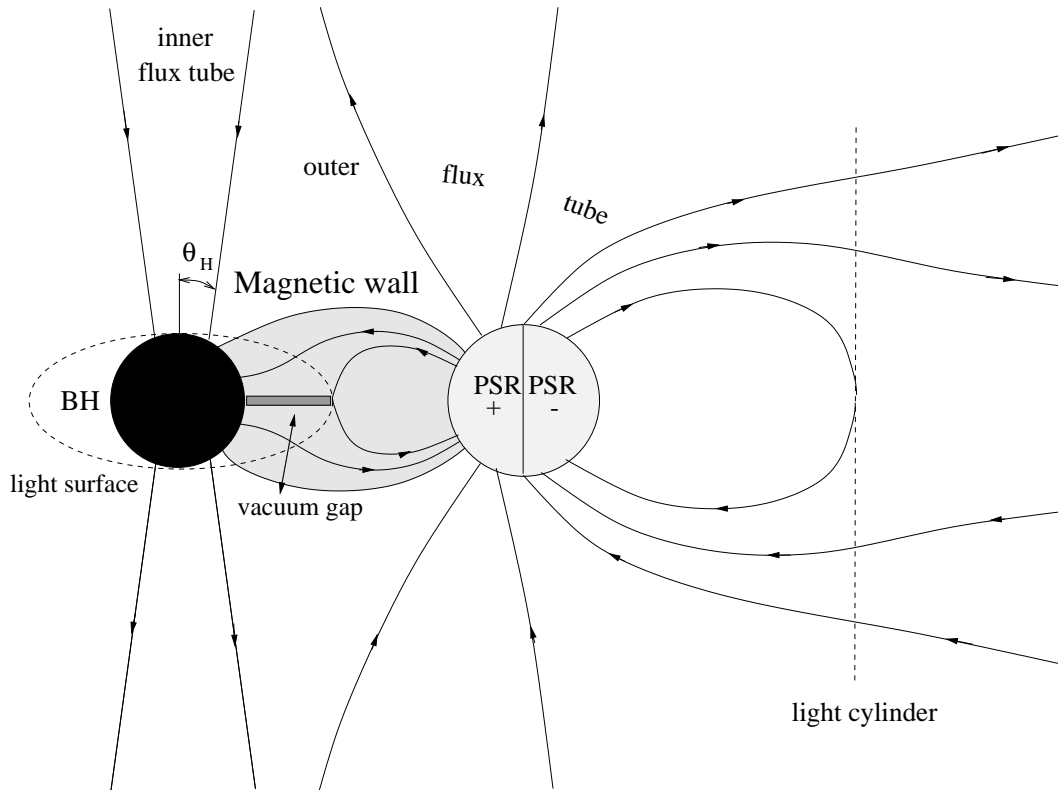


Figure 5: Schematic illustration of the poloidal topology of the magnetosphere of a torus surrounding a rapidly rotating black hole. The direct link between the inner torus magnetosphere and the horizon results in energy and angular momentum transfer from the black hole to the torus. This input is catalyzed by the torus into gravitational radiation, winds, thermal and MeV neutrino emissions. The associated Maxwell stresses are mediated by poloidal currents, which close over a current sheet (marked as vacuum gap) in an annulus of vanishing magnetic field (as indicated). A baryon-poor inner flux-tube serves as an artery for a *minor* fraction of black hole-spin energy. The inner and outer flux tubes are separated by a charge and current sheet in the outflow section. The dashed lines indicate the inner and outer light cylinders. The lifetime of the system is set by the lifetime of rapid spin of the black hole. Reprinted from van Putten & Levinson ApJ 584, 937 (2003).

with a uniformly magnetized surface of the torus.

Like in pulsars (Goldreich & Julian 1969; Michel 1982), the vacuum magnetosphere of the rotating torus is unstable. By vacuum break-down, the flux-surfaces will evolve with electric charges to a largely force-free state. As a result, a magnetosphere develops which consists of conductive flux-surfaces and magnetic winds. This is shown schematically in fig 5. In the limit of infinite torus conductivity, the flux-surfaces in the outer/inner torus magnetosphere assume rigid corotation with the outer/inner face of the torus. A transonic inflow is expelled from the inner face along the open field lines to the horizon. For a rapidly rotating black hole we anticipate $\Omega_T < \Omega_H$, and so energy and angular momentum are transferred from the hole into the inner face of the torus (see section 2.7), tending to spin it up. Likewise, a transonic outflow is ejected from the outer face to infinity, resulting in a loss of energy and angular momentum of the outer face. A quasi steady-state is quickly reached, whereby a flow of angular momentum mediated by shear forces between the differentially rotating torus layers is established (van Putten & Ostriker 2001). The energy deposited in the torus is emitted predominantly in the form of gravitational waves, owing to large deformations of the torus, as well as MeV neutrinos and baryon rich winds to infinity, resulting from the rapid heating of the torus by the friction between its layers (van Putten & Levinson 2003). This is one of the major differences between the open-and-closed- field geometries.

When the magnetic field strength inside the torus exceeds a few time 10^{15} G it becomes dynamically important. It is then anticipated that magnetic stresses that builds up inside the torus will lead to nonlinear, dynamical deformations of the torus. The power spectrum of the induced mass moments is likely to be dominated by the several lowest multipoles. A naive estimate of the field strength above which the torus becomes unstable to deformations may be obtained by equating the torque acting on a perturb current ring, owing to the mutual magnetic interaction between the two current rings, with the gravitational torque exerted by the central black hole (van Putten & Levinson 2003). This yields a critical field strength of about 10^{16} G. The presence of toroidal field components inside the torus may somewhat alter this estimate. Interestingly, this critical magnetic field corresponds to a spin down time of the order of tens of seconds for a stellar mass black hole, consistent with durations of long GRBs. Full 3D GRMHD simulations are ultimately needed to study the dynamics of the torus (including the back-reaction of the black hole) in this regime. Using a toy model, Bromberg et al. (2005) have recently calculated the evolution of the mass moments of the deformed torus. Their simulations reveal the existence of a nonlinear, oscillatory phase that sets in when the magnetic field approaches the critical value. The duration of this phase is found to be very long compared with the orbital period, for a certain range of parameters. The deformations of the torus that result from this magnetic self-interaction should give rise to a burst of gravitational wave emission with durations of several to several tens of seconds (see Bromberg et al. 2005 for analysis of the gravitational wave spectrum). For reasonable parameters

we anticipate such sources to be detectable by LIGO and VIRGO out to a distance of 100 Mpc and even larger (van Putten et al. 2004)

The powerful wind driven by the pressure gradients in the surface layers of the hot torus passes through the outer Alfvén point. This results in the opening of some magnetic field lines in the outer layers of the inner torus magnetosphere. Because the torus is rotating and magnetized, the ejection of the wind is partially anisotropic. Specifically, mass flux is generally suppressed along magnetic field lines that are inclined toward the rotation axis, and enhanced along field lines that are strongly inclined away from the axis (Blandford & Payne 1982; Romanova et al. 1997), owing to centrifugal forces. The details of the outflow depend on the heating and cooling rate of the corona, and on its structure. We speculate that large pressure gradients in the corona would tend to push matter along some of the magnetic field lines originally connected to the horizon, and that a combination of buoyancy and centrifugal forces may subsequently give rise to a twist of these field lines, some of which may ultimately fold and open to form an open magnetic flux tube near the rotation axis that extends from the horizon to infinity. The resulting structure consists of two coaxial flux tubes with opposite magnetic orientation, as shown in fig 5. The inner and outer flux tubes are separated by a cylindrical current and charge sheet that accounts for the jump in the electric and magnetic fields across the interface. The lower section of the inner/outer flux-tube which connects to the horizon has, instead, a parallel orientation between the poloidal magnetic field. In the perfect MHD limit, the properties of the interface are described by jump conditions as follow from Maxwell's equations. The surface charge density is given by

$$4\pi\sigma_e = [\Omega r \sin\theta B_r] = r \sin\theta \Omega_T B_{r+} - r \sin\theta (\Omega_H/2) B_{r-}, \quad (51)$$

where B_{r+} (B_{r-}) denotes the radial magnetic field near the interface in the outer (inner) flux tube, and the poloidal and toroidal surface currents by,

$$\begin{aligned} 4\pi J^r &= [B_\phi] = \left[\frac{\Omega r \sin\theta B_r}{v^r} \right], \\ 4\pi J^\phi &= -[B_r]. \end{aligned} \quad (52)$$

The poloidal current (52) results beyond the Alfvén point, where the wind transports angular momentum outwards to infinity. The outflow in the inner tube is expected to be relativistic ($v^r = 1$). If the baryon rich outflow from the torus also becomes relativistic, then the latter equation implies that $J^r = \sigma_e c$, namely the poloidal current in the boundary layer is solely due to the outflowing surface charges. This current sheet is a potential site for reconnection of magnetic field lines, which would convert magnetic energy in the inner flux tube into kinetic energy.

4 NON-STATIONARY EFFECTS

The discussion in the preceding sections focused on static magnetospheres. The question of whether these structures are globally stable and how they evolve can

only be addressed using time dependent analysis. This is the ultimate goal of general relativistic MHD (GRMHD) simulations, that only very recently became feasible. Simple analytic analysis is nonetheless important, both to give us some insight into this complicated problem and to provide test cases for the simulations whenever possible.

There are two crucial issues that we think need to be clarified. The first one is the role of linear waves in the response of a magnetized flux tube to local changes. The second and most important one, is the role frame dragging plays in the global evolution of a force-free magnetosphere. We discuss these issues in turn in what follows.

4.1 Small amplitude waves

The system of GRMHD equations admits in general 4 types of modes - slow, Alfvén, fast and entropy, that can most easily be identified from a linear perturbation analysis in a homogeneous background. There is ample literature on the properties of those waves (for recent accounts see e.g., Anile 1989; Uchida 1997a,b; Komissarov 1999, 2002; Punsly 2001; van Putten 2004). The linear modes also define the critical surfaces of a static transonic flow as discussed in section 2.4 above. In essence, each such surface acts as a one-way membrane for waves of the corresponding type. Whenever the flow is locally perturbed, only information associated with subcritical modes can be transmitted backwards to the source. In particular, no information can be transmitted from the regions beyond the inner and outer fast critical surfaces, meaning that the horizon of a Kerr black hole is not in causal contact with the injection region. The question then arises, how information about the state of the black hole is transmitted through a magnetized flux tube.

In the force-free limit only two physical modes remain, the Alfvén and fast modes (e.g., Uchida 1997b; Komissarov 2002). As explained in section 2.5, in this limit the Alfvén surface coincides with the light cylinder, whereas the fast critical surface approaches the horizon. This fact has led Blandford (2002) to propose that changes near the horizon can be communicated by means of the fast mode, a proposal that has been questioned by Punsly (2001; 2003). Below, we re-examine this problem. The most detailed investigation of force-free waves in Kerr spacetime is presented in Uchida (1997a,b). This author derived a set of PDEs for the Lagrangian displacement of linear perturbations. Using a WKB approximation he then solved it to lowest order. His results confirm that to lowest order the fast wave is electromagnetic, in the sense that it propagates along null geodesics and is purely transverse. The Alfvén mode has, in general, a longitudinal component. It also propagates at the speed of light, but only along poloidal magnetic field lines. It is these properties of the force-free waves (see Punsly 2003) that are at the base of the causality dispute discussed in section 2.8. As we shall now argue, the response of a flux tube to changes in spacetime involves higher order effects, which are not accounted for in the lowest order geometric optical approximation. To illustrate this, consider a

static flux tube extending from the horizon of a Kerr black hole. Using eq. (43) the GJ charge density near the axis, as measured by a ZAMO, can be expressed in terms of the θ component of the ZAMO electric field as,

$$\rho_{GJ} = \frac{E_\theta}{2\pi\tilde{\omega}}, \quad (53)$$

where $\tilde{\omega}$ is the cylindrical radius, as defined below eq. (2). Suppose now that the system is transformed from this initial state to a slightly different state, e.g., due to a change in the angular momentum of the black hole by a small amount $\delta a \ll a$. The change in the angular velocity of the flux tube, as measured by a ZAMO, will be accompanied by a change δE_θ in the electric field, and a corresponding change in the GJ charge density:

$$\delta\rho_{GJ} = \frac{\delta E_\theta}{2\pi\tilde{\omega}}. \quad (54)$$

Consequently, the perturbed GJ charge density is associated with changes on scales comparable to the dimension of the flux tube. This means that the adjustment of the magnetosphere to global changes cannot be analyzed within the framework of the geometric optical approximation, as attempted by Punsly. It is not even clear whether for such long wavelength perturbations decomposition into MHD modes is possible. To be more precise, the perturbed charge density associated with any short-wavelength disturbance of some static solution is given by $\delta\rho_e = i\mathbf{k} \cdot \delta\mathbf{E}/4\pi$, where \mathbf{k} is the corresponding wave vector. Thus, any changes in the charge density required for adjustments of the angular velocity of an evolving magnetic flux tube would appear only to order $(k\tilde{\omega})^{-1}$, which is neglected in the lowest order geometric optical approximation. The fact that the fast mode is purely transverse to lowest order does not by itself imply that a force-free magnetosphere cannot respond to changes beyond the inner light cylinder. It simply means that account of higher order terms in the linear perturbation analysis is mandatory for exploring such effects. Such an attempt is presented in (Levinson 2004), who confirms that to lowest order the fast mode is indeed electromagnetic. However, he finds (but cf. Punsly 2004) that to second order the fast mode have a longitudinal component, and that the perturbed electric charge density beyond the light cylinder approaches $\delta\rho_{GJ}$, as given in eq. (54).

4.2 The frame dragging dynamo

To gain some insight into the role of frame dragging in the evolution of a force-free flux tube, let us first express Faraday law in terms of the ZAMO fields B_ϕ , E_r , and E_θ , and the potential A_ϕ , which will be used as our free variables. In Boyer-Lindquist coordinates eq (5) gives,

$$B_{\phi,t} + \frac{\sqrt{\Delta}}{\rho^2}(\rho\alpha E_\theta)_{,r} - \frac{1}{\rho^2}(\rho\alpha E_r)_{,\theta} = \frac{\sqrt{\Delta}}{\rho^2}(\beta_{,r}A_{\phi,\theta} - \beta_{,\theta}A_{\phi,r}). \quad (55)$$

The term on the R.H.S of the last equation, which is absent in flat spacetime, represents the effect of frame dragging. As seen it only couples to the poloidal magnetic field, and can be interpreted as a driver or a dynamo term. This term cannot be gauged away owing to the fact that frame dragging is differential. Physically, this can be attributed to the fact that the angular velocity of a ZAMO depends on radius, and so magnetic surfaces appear to be in differential rotation in the ZAMO frame, thereby giving rise to a potential drop along magnetic surfaces that tends to be screened out when sufficient plasma is present. Let us explore further the role of this driving term in the evolution of a flux tube.

Consider the evolution of a force-free magnetosphere of a slowly rotating black hole. To derive the equations for the evolving electromagnetic field, we linearize Maxwell equations (4) and (5), using the hole angular momentum a as the small parameter. We suppose that initially the magnetosphere is non-rotating, and that the magnetic field can be described by the vacuum Wald solution (Wald 1974). To second order in a/M the initial solution reads:

$$A_\phi = (B/2)r^2 \sin^2 \theta, \quad (56)$$

$B_\phi = E_r = E_\theta = 0$. To this order the force-free condition (40) reduces to

$$\sqrt{\Delta} j_r = -r \cot \theta j_\theta, \quad (57)$$

$$\sqrt{\Delta} E_\theta = r \cot \theta E_r, \quad (58)$$

where j_a denotes the components of the ZAMO poloidal current, which are related to the Boyer-Lindquist current through: $j_r = (\rho/\sqrt{\Delta})j^r$, $j_\theta = \rho j^\theta$. The r and θ components of eq. (4) yield,

$$-E_{r,t} + \frac{\alpha}{\rho \sin \theta} (\sin \theta B_\phi)_{,\theta} = 4\pi \alpha j_r, \quad (59)$$

$$E_{\theta,t} + \frac{\alpha}{\rho} (B_\phi)_{,r} = -4\pi \alpha j_\theta, \quad (60)$$

From equations (55) - (60), we obtain a differential equation for the electric field E_θ (see Levinson 2004 for further details):

$$(1 + \Delta \tan^2 \theta / r^2) E_{\theta,tt} + \frac{\sqrt{\Delta}}{r^2} (\sqrt{\Delta} B_{\phi,t})_{,r} - \frac{\Delta}{r^3 \cos \theta} (\sin \theta B_{\phi,t})_{,\theta} = 0, \quad (61)$$

with

$$B_{\phi,t} = \frac{\sqrt{\Delta}}{r^2} \left[-(\sqrt{\Delta} E_\theta)_{,r} + \frac{\sqrt{\Delta}}{r} (\tan \theta E_\theta)_{,\theta} - \frac{6M Ba}{r^2} \sin \theta \cos \theta \right]. \quad (62)$$

The last term on the R.H.S of eq. (62) accounts for the differential frame dragging of the initial magnetic field, that is, $\beta_{,r} A_{\phi,\theta} - \beta_{,\theta} A_{\phi,r} = -(6M Ba/r^2) \sin \theta \cos \theta$ to second order in a/M . Now, since the magnetosphere is initially non-rotating, no

electric current is flowing in the system, viz., $j_r(t=0) = j_\theta(t=0) = 0$. To examine how the poloidal current is generated, we take the time derivative of eq. (59), and employ equations (61) and (62) to obtain near the rotation axis (that is, at small angles),

$$j_{r,t}(t=0) \simeq -12BMa \frac{\sqrt{\Delta}}{r^5} \cos^2 \theta. \quad (63)$$

Consequently, the poloidal current is driven solely by the frame dragging dynamo; the only assumption being made is that there is sufficient plasma in space to allow the condition $\mathbf{E} \cdot \mathbf{B} = 0$ to be satisfied everywhere. Note that the poloidal current is generated initially everywhere in space and not only on the horizon, in contrast to the case of a Faraday disk, as in Punsly's (2001) waveguide model (cf. Komissarov 2003). This clearly shows that the interpretation of the horizon as a unipolar inductor is inappropriate; it is the gravitomagnetic effect that is responsible for the adjustment of the magnetosphere to changes. A similar conclusion was drawn earlier by Komissarov (2003, 2004b). Equation (61) is rather complicated. Approximate, analytic solutions can be obtained near the horizon (Levinson 2004)⁵. For the case considered here we obtain in the region where $\alpha \ll 1$, and for times $t < 2M \ln(2M^2/\Delta)$:

$$E_\theta = \frac{3Ba}{8M^2} \sqrt{\Delta} \sin 2\theta [\cosh(t/2M) - 1], \quad (64)$$

$$B_\phi = -\frac{3Ba}{8M^2} \sqrt{\Delta} \sin 2\theta \sinh(t/2M), \quad (65)$$

$$j_r = -\frac{3Ba}{4M^3} \sqrt{\Delta} \cos^2 \theta \sinh(t/2M). \quad (66)$$

As seen, the perturbed force-free field grows exponentially with an e-folding time $2M$. Note that after time $t \sim 2M \ln(2M^2/\Delta)$, at which the above solution is no longer valid, the toroidal magnetic field and the current evolve close to their steady-state values, viz., $B_T \sim (\Omega_H/2)F_{\phi\theta} \sin \theta$, $I = B_T/2$. We conjecture that after this time the system will reach a steady state. This suggests that the magnetosphere inside the ergosphere evolves to a steady-state solution over a few dynamical times.

4.3 Numerical Simulations

There have been several attempts in recent years to perform numerical simulations of the Blandford-Znajek process. They all show the tendency of the magnetosphere to evolve towards a stable steady state. In the GRMHD simulations reported in Koide et al. (2002) and Koide (2003), the initial magnetic field configuration is described by the Wald solution. The plasma around the black hole has initially zero momentum, a uniform mass density, and Alfvén velocity of 0.983 c (Koide 2003).

⁵There is a typo in eq. (24) of Levinson (2004). It should read: $B_{T,\tau} = x2M^2 \sin \theta (f_0 - \frac{3Ba}{8M^2} \sin 2\theta)$.

This initial condition is similar to the one invoked in section 4.2, except that plasma inertia is not neglected and the black hole in the simulations is nearly maximally rotating. The simulations clearly show the generation of a toroidal magnetic field by the frame dragging dynamo inside the ergosphere, and the consequent decrease of the specific energy of the plasma until it becomes negative. The twist of the magnetic field lines seems to be propagating outward, carrying energy and angular momentum on account of the black hole rotational energy. The simulations reported in Koide et al. (2002) run for a time of about several r_s/c after which the code crashes. This run is, unfortunately, not sufficiently long for the system to reach a steady-state. Nonetheless, it does show that the magnetosphere inside the ergosphere evolves over a few dynamical times, consistent with the analytic result derived in section 4.2. Komissarov (2001) performed 2D, time dependent numerical simulations of the evolution of a force-free, axisymmetric monopole configuration around a Kerr black hole. He found that the solution quickly settles to a stable steady state, with the angular velocity of magnetic field lines approaching $\Omega_H/2$ (meaning maximum extraction efficiency), thereby confirming the results of BZ. He later generalized the numerical model to include inertial terms (Komissarov 2004a), and demonstrated that the inertia of the plasma near the event horizon is dynamically unimportant, and that the force-free limit is a good approximation for magnetically dominated flows, at least for the monopole case. The simulations also show the development of a double transonic flow that extends beyond the outer fast critical surface. In a later paper (Komissarov 2004b), this author explored more realistic configurations. He also included a prescription for electric resistivity that enabled him to incorporate dissipative magnetospheric regions (current sheets) in the numerical model. He confirms his earlier conclusions, that a stable steady state is reached whereby energy is extracted electromagnetically. He finds, however, that in certain magnetospheric configurations, current sheets may form on the equatorial plane. Such regions may provide a path for the return current of the global circuit. Moreover, in certain cases collimation of the outflow is not seen up to a few tens of gravitational radii.

In another set of numerical experiments (Hirose et al. 2004; McKinney & Gammie, 2004; De Villiers et al. 2005), the evolution of a weakly magnetized torus surrounding a Kerr black hole has been examined. It is generally found that the magnetic field in the torus is initially amplified via the MRI and becomes turbulent. A funnel region near the rotation axis of the hole is identified in those simulations, in which the magnetic field appears to be ordered and nearly force-free. This region is well described by the BZ model (McKinney & Gammie, 2004), and it appears that energy is being extracted along those force-free flux tubes. However, the overall energy flux (integrated over the horizon) is dominated by the enthalpy of accreted plasma. This is not surprising in view of the initial and boundary conditions invoked. Nonetheless, the presence of a magnetically dominated polar region along which a significant fraction of the accreted energy is channeled into a Poynting flux jet is interesting and of direct astrophysical relevance.

The conclusion to be drawn from the numerical experiments described above is that the magnetosphere of a Kerr black hole is a stable, causal structure, and that its evolution is driven by the frame dragging dynamo.

5 CONCLUSION

- The system of static, axisymmetric ideal MHD equations in Kerr geometry is characterized by five quantities conserved along magnetic flux surfaces; the specific energy and angular momentum, the angular velocity of magnetic lines, the ratio of particle and magnetic fluxes, and the entropy. The stream function that defines those flux surfaces obeys a second order, nonlinear PDE that involves the five invariants.
- The specific energy of a given magnetic surface that extends down to the horizon becomes negative when two conditions are satisfied: (i) its angular velocity is larger than zero and smaller than that of the black hole, and (ii) the corresponding Alfvén point is located inside the ergosphere. Energy and angular momentum can be transmitted from the horizon outwards along such a negative energy flux tube, on account of the black hole rotational energy. The rate at which energy is extracted from the hole depends on the strength of the magnetic field near the inner fast critical surface, and the angular velocity of the flux tube. For typical astrophysical parameters, the total power that can be extracted is sufficient to account for the luminosities exhibited by relativistic systems, e.g., AGNs, GRBs, microquasars, provided the efficiency is high.
- Transonic solutions must pass through several singular surfaces. Of most interest are the slow magnetosonic, Alfvén and fast magnetosonic surfaces, on which the bulk velocity of the flow equals the velocity of the corresponding linear mode. There are two sets of such critical surfaces, the inner one associated with a transonic inflow into the hole, and an outer one associated with a transonic outflow to infinity. Each surface acts as a one-way membrane to the corresponding mode, and determines what information can be communicated backward to the injection region. The entire structure of the flow is determined by appropriate boundary conditions and the regularity conditions on the critical surfaces. This is true also in the limit of zero inertia.
- Double transonic structures that extend from the horizon to beyond the outer fast critical surface, as in the applications to astrophysical jets, must contain a region where the ideal MHD condition is violated. This region serves as a plasma source and must be located somewhere between the inner and outer Alfvén surfaces. The global double-transonic flow structure is controlled entirely by the micro-physical conditions in the plasma source and the regularity conditions. In the force-free case the deviation from force-freeness in the

plasma source may be very small, and in any case is required only to ensure the continuity of electric current along magnetic field lines. In some configurations, as in the closed-field geometry discussed in section 3.2, a cylindrical current sheet may separate the inner, double transonic flow and the outer magnetosphere.

- The extracted energy may be released through various channels, depending on the global structure of the magnetosphere. In open-field magnetospheres, where there is no direct link between the black hole and the surrounding disk, the extracted energy is ultimately channeled along the rotation axis in the form of a Poynting flux dominated outflow. In closed-field magnetospheres, a significant fraction of magnetic field lines that penetrate the horizon are anchored to the surrounding torus. In such configurations the major fraction of the extracted energy is transferred to the torus, and only about 0.1 % are channeled along the rotation axis. The energy deposited into the torus may result in strong gravitational wave emission and baryon rich winds. The ram pressure of the baryon rich wind that ensheath the inner jet can provide a means for collimating the inner jet.
- The global evolution of a magnetosphere is governed by frame dragging. It is the fact that the ZAMO angular velocity varies with radius that causes the appearance of field-aligned electric field in vacuum (or a starved magnetosphere more generally). In regions where sufficient plasma is present the parallel electric field tends to be screened out. The adjustment of the electric charge to changes in spacetime is instantaneous essentially, and is dictated solely by the requirement that the condition $\mathbf{E} \cdot \mathbf{B} = 0$ is preserved in the course of evolution. The term $\hat{\mathbf{m}}\mathbf{B} \cdot \nabla\beta$ that appears in the homogeneous Maxwell equations, where \mathbf{B} is the ZAMO poloidal magnetic field, $-\beta$ is its angular velocity, and $\hat{\mathbf{m}}$ is a unit vector in the ϕ direction, can be treated as a driving term that generates the toroidal magnetic field and poloidal electric current.

ACKNOWLEDGMENT

I thank J. Bekenstein, V. Beskin, S. Komissarov, Y. Lyubarsky, J.C. McKinney, and M. van Putten for useful comments. This work was supported by an ISF grant for the Israeli Center for High Energy Astrophysics

References

- [1] Anile, A.M. Relativistic Fluids and Magnetofluids; Cambridge Univ. Press: Cambridge, 1989

- [2] Begelman, M.C.; Blandford, R.D.; Rees, M.J. *Rev. Mod. Phys.* 1984, 56, 255-351
- [3] Bekenstein, J.D.; Oron, E. *Phys. Rev. D.* 1978, 18, 1809-1820
- [4] Beskin, V.S. *Phys. Uspekhi*, 1997, 40, 659-688
- [5] Beskin, V.S.; Kuznetsova, I.V. *Nuovo Cimento B* 2000, 115, 795-815
- [6] Beskin, V.S.; Parèv, V.I. *Phys. Uspekhi* 1993, 36 529
- [7] Bisnovatyi-Kogan, G.S.; Ruzmaikin, A.A. *Astrophys. Space Sci.* 1976, 42, 401-424
- [8] Blandford, R.D. *Prog. Theor. Phys. Suppl.* 2001, 147, 182
- [9] Blandford, R.D. in *Lighthouses of the Universe*, Gilfanov, M.; Sunyaev, R.A.; Churazov, E.; Springer: NY, 2002, 381-406
- [10] Blandford, R.D. *Mon. Not. Roy. Astron. Soc.*, 1976, 176, 465-481
- [11] Blandford, R.D.; Levinson, A. *Astrophys. J.* 1995, 441, 79-95
- [12] Blandford, R.D.; Payne, D.G. *Mon. Not. Roy. Astron. Soc.* 1982, 199, 883-903
- [13] Blandford, R.D.; Znajek, W.L. *Mon. Not. Roy. Astron. Soc.*, 1977, 179, 433-456
- [14] Braithwaite, J., & Spruit, H.C. *Nature*, 2004, 431, 819-821
- [15] Bromberg, O.; Levinson, A.; van Putten, M.V.P. *Astrophys. J.*, 2005, submitted
- [16] Brown G.E.; Lee, C.-H.; Wijers, R.A.M.J.; Lee, H.K.; Israelian, G.; Bethe, H.A. *New Astron.* 2000, 5, 191-210
- [17] Camenzind, M. *Astron. Astrophys.* 1986, 162, 32-44
- [18] Celotti, A. in *Relativistic Jets in AGN*, Ostrowski, M.; Sikora, M.; Madejski G.; Begelman, M. 1997, 270-278
- [19] Dermer, C.; Schlickeiser, R. *Astrophys. J.* 1993, 416, 458-484
- [20] De Villiers, J.; Hawley, J.F.; Krolik, J.H.; Hirose, S. *astro-ph/0407092*, 2005
- [21] Duncan, R.C.; Thompson, C. *Astrophys. J.* 1992, 392, L9-L13
- [22] Eichler, D., *Astrophys. J.* 1982, 254, 683-687
- [23] Eichler, D.; et al. *Nature* 1989, 340, 126-128
- [24] Fendt, C. *Astron. Astrophys.* 1997, 319, 1025-1035

- [25] Flowers, E., & Ruderman, M. *Astrophys. J.* 1977, 215, 302-310
- [26] Ghosh, P. *Mon. Not. Roy. Astron. Soc.* 2000, 315, 89-97
- [27] Ghosh, P.; Abramowicz, M.A. *Mon. Not. Roy. Astron. Soc.* 1997, 292, 887-895
- [28] Goldreich, P.M.; Julian, W.H. *Astrophys. J.* 1969, 157, 869-880
- [29] Hirose, S.; Krolik, J.H.; De Villiers, J.; Hawley, J.F. *Astrophys. J.* 2004, 606, 1083-1097
- [30] Hirotani, K.; Takahashi, M.; Nitta, S.; Tomimatsu, A. *Astrophys. J.* 1992, 386, 455-463
- [31] Kerr, R.P. *Phys. Rev. Lett.* 1963, 11, 237-238
- [32] Kirk, J.G.; Lyubarsky, Y. *Publ. Astron. Soc. Austr.* 2001, 18, 415-420
- [33] Koide, S.; Shibata, K.; Kudoh, T.; Meier, D. *Science* 2002, 295, 1688-1691
- [34] Koide, S., 2003, *Phys. Rev. D.*, 67, 104010-104025
- [35] Komissarov, S.S., *Mon. Not. Roy. Astron. Soc.* 1999, 303, 343-366
- [36] Komissarov, S.S., *Mon. Not. Roy. Astron. Soc.* 2001, 326, L41-L44
- [37] Komissarov, S.S., *Mon. Not. Roy. Astron. Soc.* 2002, 336, 759-766
- [38] Komissarov, S.S., *Mon. Not. Roy. Astron. Soc.* 2003, 341, 717-720
- [39] Komissarov, S.S., *Mon. Not. Roy. Astron. Soc.* 2004a, 350, 1431-1436
- [40] Komissarov, S.S., *Mon. Not. Roy. Astron. Soc.* 2004b, 350, 427-448
- [41] Kouveliotou, C.; Duncan, R.C.; Thompson, C. *Scientific American* 2003, 34-41
- [42] Lee, H.K.; Brown, G.E.; Wijers, R.A.M.J. *Astrophys. J.* 2000, 536, 416-419
- [43] Lee, H.K.; Lee, H.C.; van Putten, H.P.M. *Mon. Not. Roy. Astron. Soc.* 2001, 324, 781-784
- [44] Levinson, A. *Astrophys. J.* 1996, 467, 546-550
- [45] Levinson, A. *Astrophys. J.* 1998, 507, 145-155
- [46] Levinson, A. *Astrophys. J.* 2004, 608, 411-417
- [47] Levinson, A.; Blandford, R.D. *Astrophys. J.* 1996, 456, L29- L32
- [48] Levinson, A.; Eichler D. *Astrophys. J.* 1993, 418, 386-390

- [49] Levinson, A.; Eichler D. *Phys. Rev. Lett.* 2000, 85, 236-239
- [50] Levinson, A.; et al. *Astrophys. J.* 2002, 576, 923-931
- [51] Lovelace R.V.E. *Nature* 1976, 262, 649-652
- [52] Lyubarsky, Y. *Mon. Not. Roy. Astron. Soc.* 2003, 345, 153-160
- [53] Macdonald, D. A. *Mon. Not. Roy. Astron. Soc.* 1984, 211, 313-329
- [54] Macdonald, D. A.; Thorne, K. S. *Mon. Not. Roy. Astron. Soc.* 1982, 198, 345-382
- [55] Mannheim, K. *Astron. Astrophys.* 1993, 269, 67-76
- [56] Markey, P., & Tayler, R.J. *Mon. Not. Roy. Astron. Soc.* 1973, 163, 77-91
- [57] McKinney, J.; Gammie, C.F. *Astrophys. J.* 2004, 611, 977-995
- [58] Mestel, L. *Stellar Magnetism*, Clarendon Press: Oxford, 1999
- [59] Meszaros, P.; Rees, M.J. *Astrophys. J.* 1997, 482, L29-L32
- [60] Michel, F. C. *Rev. Mod. Phys.* 1982, 54, 1-66
- [61] Nitta, S-Y.; Takahashi, M.; Tomimatsu A. *Phys. Rev. D.* 1991, 44 2295-2305
- [62] Paczyński, B.P., 1991, *Acta Astron.*, 41, 257-267
- [63] Phinney, E.S. in *Astrophysical Jets*; Ferrari, A.; Pacholczy, A.G. Dordrecht: Reidel, 1983, 201-213
- [64] Punsly, B. *Black Hole Gravitohydromagnetics*, Springer-Verlag: Berlin, 2001
- [65] Punsly, B. *Astrophys. J.* 2003, 583, 842-852
- [66] Punsly, B. *Astrophys. J.* 2004, 612, L41-L44
- [67] Punsly, B.; Coroniti, F.V. *Astrophys. J.* 1990, 350, 518-535
- [68] Romanova, L.L.; Lovelace, R.V.E. *Astron. Astrophys.* 1992, 262, 26-36
- [69] Romanova, L.L.; Lovelace, R.V.E. *Astrophys. J.* 1997, 457, 97-105
- [70] Romanova, M.M.; Ustyugova, G.V.; Koldoba, A.V.; Chechetkin, V.M.; Lovelace, R.V.E. *Astrophys. J.* 1997, 482, 708-711
- [71] Ruffini, R.; Wilson, J.R. 1975, *Phys Rev D*, 12, 2959-2962
- [72] Sikora, M.; Begelman, M.; Rees, M. *Astrophys. J.* 1994, 421, 153-162

- [73] Takahashi, M.; Nita, S.; Tatematsu, Y.; Tominatsu, A. *Astrophys. J.* 1990, 363, 206-217
- [74] Thompson, D. J.; et al. *Astrophys. J.* 1993, 415, L13-L16
- [75] Thomson, C. in *Relativistic Jets in AGN*, Ostrowski, M.; Sikora, M.; Madejski G.; Begelman, M. 1997, 63-84
- [76] Thomson, C.; Duncan, R.C. *Astrophys. J.* 1993, 408, 194-217
- [77] Thorne, K.S.; Price, R.H.; Macdonald, D.A. *Black Holes: The Membrane Paradigm*; Yale Univ. Press: NH, 1986
- [78] Uchida, T. *Mon. Not. Roy. Astron. Soc.* 1997a, 286, 931-947
- [79] Uchida, T. *Mon. Not. Roy. Astron. Soc.* 1997b, 291, 125-144
- [80] Uzdensky, D. A. *Astrophys. J.* 2004a, 603, 652-662
- [81] Uzdensky, D. A. *Astrophys. J.* 2004b, in press (astro-ph/0410715)
- [82] van Putten, M.H.P.M. *Science* 1999, 284, 115-118
- [83] van Putten, M.H.P.M. *Phys. Rev. Lett.* 2000, 84, 3752-3755
- [84] van Putten, M.H.P.M. *Phys. Rep.*, 2001, 345, 1-59
- [85] van Putten, M.H.P.M., 2002, *ApJ*, 575, L71-L74
- [86] van Putten, M.H.P.M. *Gravitational radiation, luminous black holes and gamma-ray burst supernovae*, Cambridge Univ. Press: Cambridge, 2004 (in press)
- [87] van Putten M.H.P.M.; Levinson, A. *Astrophys. J.* 2001, 555, L41-L44
- [88] van Putten M.H.P.M.; Levinson, A. *Science* 2002, 295, 1874-1877
- [89] van Putten M.H.P.M.; Levinson, A. *Astrophys. J.* 2003, 584, 937-953
- [90] van Putten M.H.P.M.; Ostriker, E.C. *Astrophys. J.* 2001, 552, L31-L34
- [91] van Putten M.H.P.M.; et al. *Phys. Rev. D.* 2004, 69, 1-21
- [92] Wald, R.M. *Phys. Rev. D.* 1974, 10(6), 1680-1685
- [93] Weber, E.j.; Davis, L. Jr. *Astrophys. J.* 1967, 148, 217-227
- [94] Wilms, J.; et al. *Mon. Not. Roy. Astron. Soc.* 2001, 328, L27-L31
- [95] Woosley, S.E. *Astrophys. J.* 1993, 405, 273-277
- [96] Znajek, R. L. *Mon. Not. Roy. Astron. Soc.* 1977, 179, 457-472